Marine Geophysical Researches **22:** 235–250, 2001.

Bathymetric Map of the Gorda Plate: Structural and Geomorphological Processes Inferred from Multibeam Surveys

Robert P. Dziak[1,*], Christopher G. Fox[2], Andra M. Bobbitt[1] and Chris Goldfinger[3]
[1]*Oregon State University, Cooperative Institute for Marine Resources Studies, Hatfield Marine Science Center, Newport, Oregon, 97365, USA;* [2]*National Oceanic and Atmospheric Administration/Pacific Marine Environmental Laboratory, Hatfield Marine Science Center, Newport, Oregon, 93765, USA;* [3]*College of Oceanic and Atmospheric Sciences, Oregon State University, Corvallis, Oregon, USA;* **Author for correspondence (Tel.: 541-8670175; Fax: 541-8673907; E-mail: dziak@pmel.noaa.gov)*

Received 28 September 2000; accepted 4 July 2001

Key words: Gorda Plate, bathymetric maps, structural deformation, submarine canyons

Abstract

Full-coverage multibeam bathymetric maps of the southern section of the Juan de Fuca Plate, also known as the Gorda Plate, are presented. The bathymetric maps represent the compilation of multibeam surveys conducted by the National Oceanic and Atmospheric Administration during the last 20 yrs, and illustrate the complex tectonic, volcanic, and geomorphologic features as well as the intense deformation occurring within this region. The bathymetric data have revealed several major, previously unmapped midplate faults. A series of gently curving faults are apparent in the Gorda Plate, with numerous faults offsetting the Gorda Plate seafloor. The multibeam surveys have also provided a detailed view of the intense deformation occurring within the Gorda Plate. A preliminary deformation model estimated from basement structure is discussed, where the southern part of the plate (south of $\sim 42°30'$ N) seems to be deforming through a series of left-lateral strike-slip faults, while the northern section appears to be moving passively with the rest of the Juan de Fuca Plate. The bathymetry also demonstrates the Mendocino and Eel Canyons are prominent morphologic features in the northern California margin. These canyons are active depositional features with a large sediment fan present at the mouths of both the Mendocino and Eel canyons. The depositional lobes of these fan(s) are evident in the bathymetry, as are the turbidite channels that have deposited sediment along the fans over time. The Trinidad Canyon is readily evident in the margin morphology as well, with a large (∼10 km) plunge pool formed at the mouth of the canyon as it enters the Gorda Plate sediments.

Introduction

During the 1990s, the results of extensive bathymetric surveys covering large areas of the seafloor have been published in *Marine Geophysical Researches* as large-scale maps (Scheirer et al., 1996; Cochran et al., 1993; Macdonald et al., 1992; Purdy et al., 1990). These studies made it possible to widely disseminate the detailed results of these surveys; however these previous bathymetric studies all have focused on various parts of the global Mid-Ocean Ridge system. In this paper, we present fold-out maps of the Gorda Plate, the highly faulted section of southern Juan de Fuca Plate from 40.5°–43.5° N and 128°–124.5° W (Figure 1). These bathymetric maps represent the compilation of several SeaBeam surveys conducted during the 1980s and 1990s by the National Oceanic and Atmospheric Administration's National Ocean Service and Vents Program. The most recent survey was done in October of 1997 using SeaBeam 2100 on the NOAA Ship *Ronald H. Brown*. The 1997 survey lasted 14 days and mapped the remaining 75% of the plate not covered by previous surveys. This is the first time that a full coverage bathymetric survey has been done of an entire microplate from the source ridge to the termination at the subduction zone.

The Juan de Fuca (JdF) Plate is the location of the first magnetic anomaly evidence in the Pacific Ocean supporting the theory of plate tectonics (Mason and Raff, 1961; Vine and Mathews, 1963; Figure 2). Modeling the internal deformation of the JdF Plate has more recently been seen as the key to understanding the complex subduction zone tectonics of the region

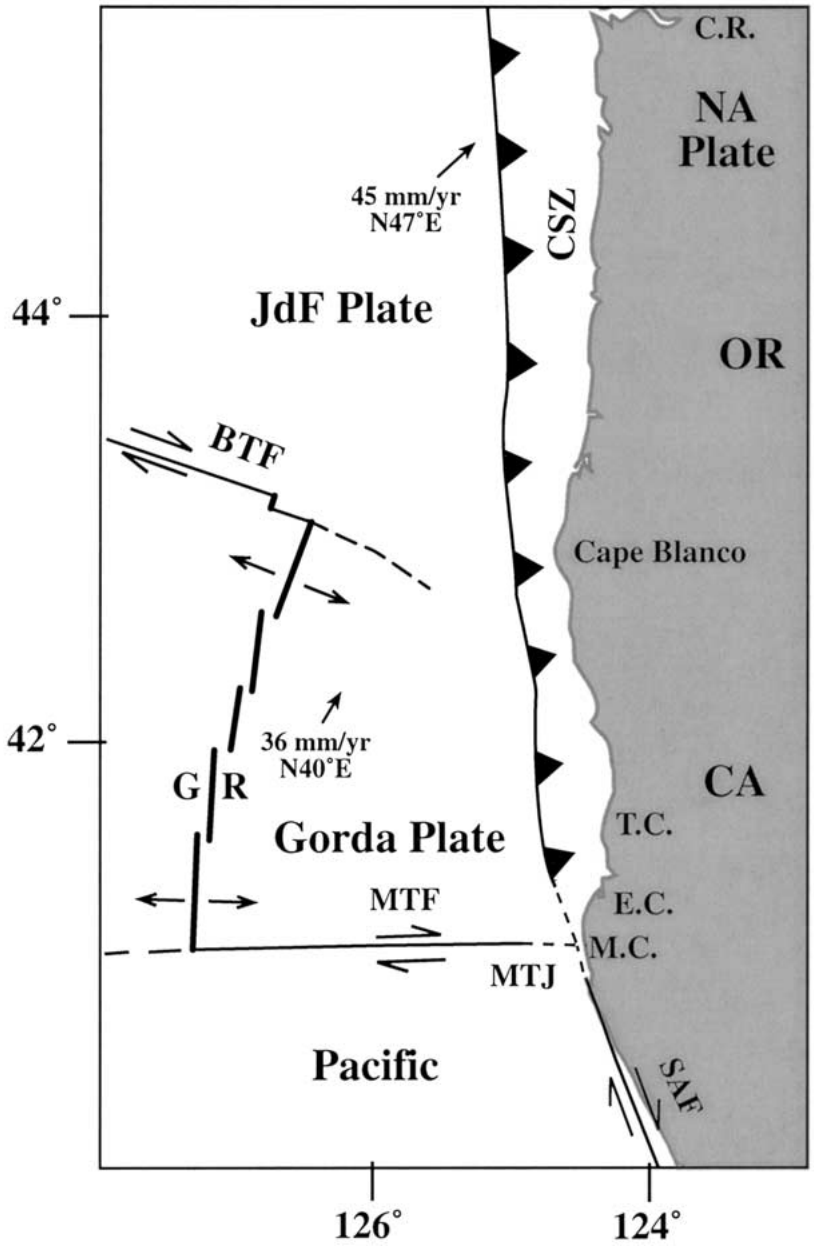

Figure 1. Location map showing the tectonic setting of the Gorda Deformation Zone (GDZ). JdF = Juan de Fuca Plate; NA = North American Plate; BTF = Blanco Transform Fault; GR = Gorda Ridge; MTF = Mendocino Transform Fault; MTJ = Mendocino Triple Junction; SAF = San Andreas Fault; C.R. = Columbia River. M.C., E.C., and T.C. show the landward location of the Mendocino, Eel, and Trinidad Canyons. CA and OR are California and Oregon, respectively. SAF, MTJ, and MFZ termini are dashed to illustrate the complexity of the triple junction region. Relative motion vectors (North American reference frame) between the western North American Plate, Juan de Fuca Plate, and Gorda Deformation Zone are given with directions and rates shown (Riddihough, 1984). The GDZ, the southern extension of the larger Juan de Fuca Plate, is extremely weak and can be considered a zone of deformation rather than a rigid tectonic plate.

Figure 2. Magnetic anomalies of the southern Juan de Fuca Ridge spreading system (after *Wilson,* 1993). DF stands for deformation front of the Cascadia Subduction Zone, the rest of the abbreviations are the same as in Figure 1. Timescale is in millions of years. Lines extending away from plate boundaries indicate locations of pseudofaults. The NNE trend of the Gorda Deformation Zone fabric can be inferred from the orientation of the magnetic anomalies east of the Gorda Ridge.

(Spence, 1989; Wang et al., 1997). In particular the southern extension of the JdF Plate, the Gorda Plate, has been the focus of various types of plate deformation research based on magnetic anomalies (Wilson, 1989, 1993), seismicity (Fox and Dziak, 1999) and structural lineations observed from GLORIA sidescan (Stoddard, 1987, 1991; Masson et al., 1988), while other work has employed finite element modeling (Denlinger, 1992). The lack of high-resolution bathymetry and the presence of systematic earthquake location error have prevented construction of deformation models that are consistent with all data sets. The new high-resolution bathymetry of the Gorda Plate presented should help refine previous deformation analyses.

Tectonic Setting

The 400 × 400 km Gorda Plate is the southern extension of the Juan de Fuca Plate, offshore southern Oregon and northern California, and is separated from the rest of the plate by the southeast trending fracture zone extension of the Blanco Transform Fault (Figure 1). The Gorda Plate is bordered to the west by the Gorda Ridge and to the south by the east-west trending Mendocino Transform Fault (both of which form the boundaries with the Pacific Plate). To the east, the Gorda Plate subducts beneath the North American plate at the rate of 36 mm/yr along the Cascadia Subduction Zone. The unstable Mendocino Triple Junction, one of the most seismically active areas in North America, lies at the southeast corner of the Gorda Plate where the San Andreas Fault, the Mendocino Transform Fault, and Cascadia Subduction Zone meet. The subduction zone along this section of the Gorda Plate has an enigmatic lack of interplate seismicity that seems at odds with paleoseismic evidence of past large earthquakes (Clarke and Carver, 1992). The small size, relatively young age (and hence thin lithosphere), and the location of the Gorda between the much larger Pacific and North American Plates means the Gorda 'Plate' is subjected to a large amount of deformation and is therefore perhaps better considered a zone of deformation than a rigid tectonic plate (Wilson, 1989). For convenience, the term 'Gorda Plate' is used in this paper to refer to the geographic feature bounded by the Gorda Ridge on the west, the Mendocino Fracture Zone on the south, and the Cascadia Subduction Zone on the east.

The small Gorda and Juan de Fuca Plates are the last remnants of the Farallon Plate, which has been steadily subducted and reduced in size to the point where the Gorda segment is undergoing severe deformation prior to its probable destruction. The Gorda Plate has long been recognized as unusual because of the severe bending of the magnetic anomalies evident in the earliest anomaly maps (Mason and Raff, 1961; Figure 2). Wilson (1989) defined the Gorda 'Deformation Zone' to be that part of the Juan de Fuca Plate south of a northwest trending line south

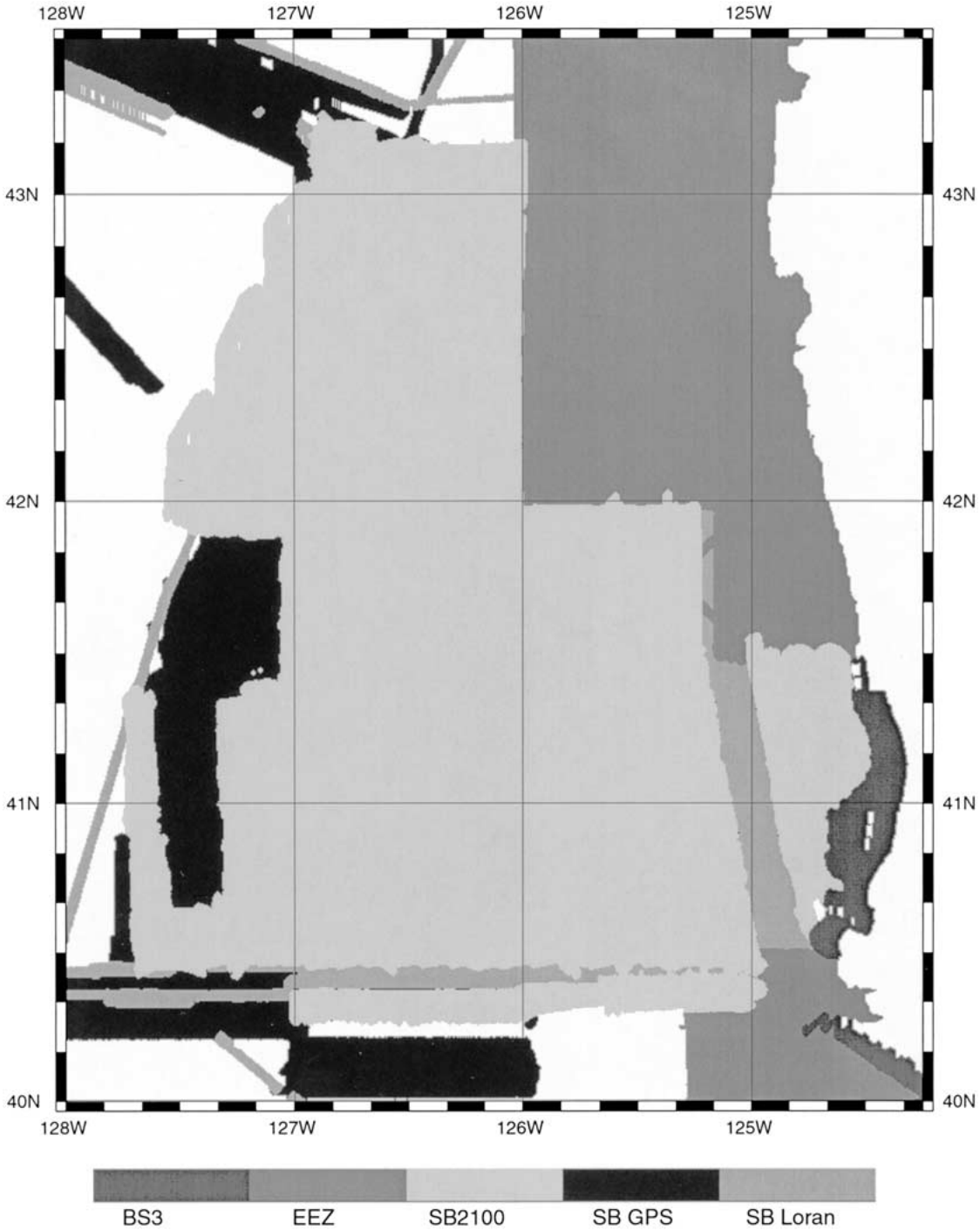

Figure 3. Diagram showing the bathymetry data coverage. Different grey scales show the major cruises (summarized in Table 1) that collected the data. SB Loran shows the area of multibeam cruises using the original 16-beam SeaBeam system and Loran-C navigation. EEZ designates the area where the original SeaBeam was employed using the shore-based RAYDIST/ARGO navigation system. BS3 shows the area where the shallow water Hydrochart II (BS^3) system on the *R/V Davidson* was utilized. SB GPS represents surveys conducted using original SeaBeam and GPS navigation. SB2100 shows the area of the single multibeam survey conducted using the SeaBeam 2100 system and GPS navigation.

of the Blanco Transform Fault. This model is based on reconstruction of rotation poles that indicate the northern Gorda Plate is moving with the Juan de Fuca Plate. The whole Gorda Plate is seismically active, exhibiting several large intraplate earthquakes during the last few decades (Lay et al., 1982; Velasco et al., 1994). The deformed magnetic lineations and predominantly strike-slip intraplate seismicity attest to internal deformation of the Gorda Plate due to north-south compression from the interaction of the Pacific and North American Plates and the obliquity of the bounding transform faults (Silver, 1971; Wilson, 1986; Smith et al., 1993).

The half-spreading rate of the Gorda Ridge changes from 2.75 cm yr^{-1} along the north near the BTF to 1.4 cm yr^{-1} along the south near the MTF. These rates were estimated from magnetic anomaly patterns over the last 2 Ma (Wilson, 1989). Prior to 2 Ma, the half-spreading rates were faster at 3–4 cm yr^{-1} and 2–3.25 cm yr^{-1} along the northern and southern sections of the ridge, respectively. The southward decrease in spreading rate is not consistent with rigid plate motion, and the difference in spreading rate through time suggests a significant change in the deformation pattern at about 2 Ma. An abrupt change in the spreading rate occurs along the ridge at $\sim 42°30'$ N. This location corresponds to a change in the strike of the Gorda Ridge and the NW-SE trending band of discordant lineations that separate the parts of the Gorda Plate that move with either the JdF Plate or the Gorda Deformation Zone (northernmost arrows, Figure 4). This NW-SE lineation boundary corresponds to a shallow basin, exhibits spreading fabric that is rotated clockwise relative to the rest of the basement lineations in the Gorda Plate, and has been proposed as a zone of right-lateral shear (Wilson, 1989). NW-SE trending right-lateral shear is in contrast to the orientation of the magnetic anomalies and basement lineations, and seems to preclude a simple interpretation of the fault geometry of the Gorda Plate.

Bathymetric Map Information

The color bathymetric foldout map (Plate 1), as well as all other color bathymetry shown in Figures 4–8, was plotted using a modified color table originally produced by W. Haxby of Lamont-Doherty Earth Observatory. The foldout map of the bathymetry was plotted with a Mercator projection at a scale of 1:750,000, and was produced using a 100-meter grid. The colors used in each of the figures showing bathymetry correspond to the same depth intervals used in Plate 1.

Data Acquisition and Processing

The multibeam bathymetry was collected from five different ships during forty-six individual cruises (Figure 3 and Table 1). The sounding data (for all surveys) were acquired using the original 16-beam SeaBeam system on the *R/V Laney Chouest*, and one of four NOAA multibeam swath mapping systems: SeaBeam (16-beam) from the NOAA Ship *Surveyor* (1980–1995), NOAA Ship *Discoverer* (1986–1995), SeaBeam 2100 (150-beam) on the NOAA Ship *Ronald H. Brown* (1997), and the shallow water Hydrochart II (BS^3) system on the NOAA Ship *Davidson* (1984, 1988). The majority of the SeaBeam swath survey data of the Gorda Plate during the 1980s was collected in support of the NOAA Exclusive Economic Zone (EEZ) Bathymetric Mapping Program. Twenty-six EEZ cruises/surveys were performed with the SeaBeam system onboard the *Surveyor* using the RAYDIST and ARGO shore-based radio navigation systems which provided ship location accuracy similar to modern GPS. Eleven other multibeam survey cruises were carried out in the 1980s aboard the *Surveyor* and *Discoverer* using Loran-C navigation. Four shallow water surveys (from 100–500 m depths) were performed in 1984 and 1988 using the Hydrochart (BS^3) system of the *Davidson* and RAYDIST/ARGO navigation. During 1994–1995, GPS navigation was available and exclusively employed in 6 surveys aboard *Laney Chouest*, *Discoverer*, and *Surveyor* (Table 1). The original SeaBeam system, however, used a simple 1500 m s^{-1} acoustic velocity hard coded into the software and it was not possible to input a more accurate sound-speed profile at the post-processing stage once the multibeam data were collected. With the advent of SeaBeam 2100 on *Ronald H. Brown*, velocity models based on direct sampling of the water column during the multibeam surveys could be input into the system. The 150-beam system mounted on *Ronald H. Brown* significantly increased the swath width of the surveys, which made it possible to cover the remaining unsurveyed 75% of the Gorda Plate in one two week cruise (Figure 3).

The two week cruise in October of 1997 aboard *Ronald H. Brown* was the first thorough test of the 2100 system installed on *Brown*, and unfortunately illuminated several problems in data collection and

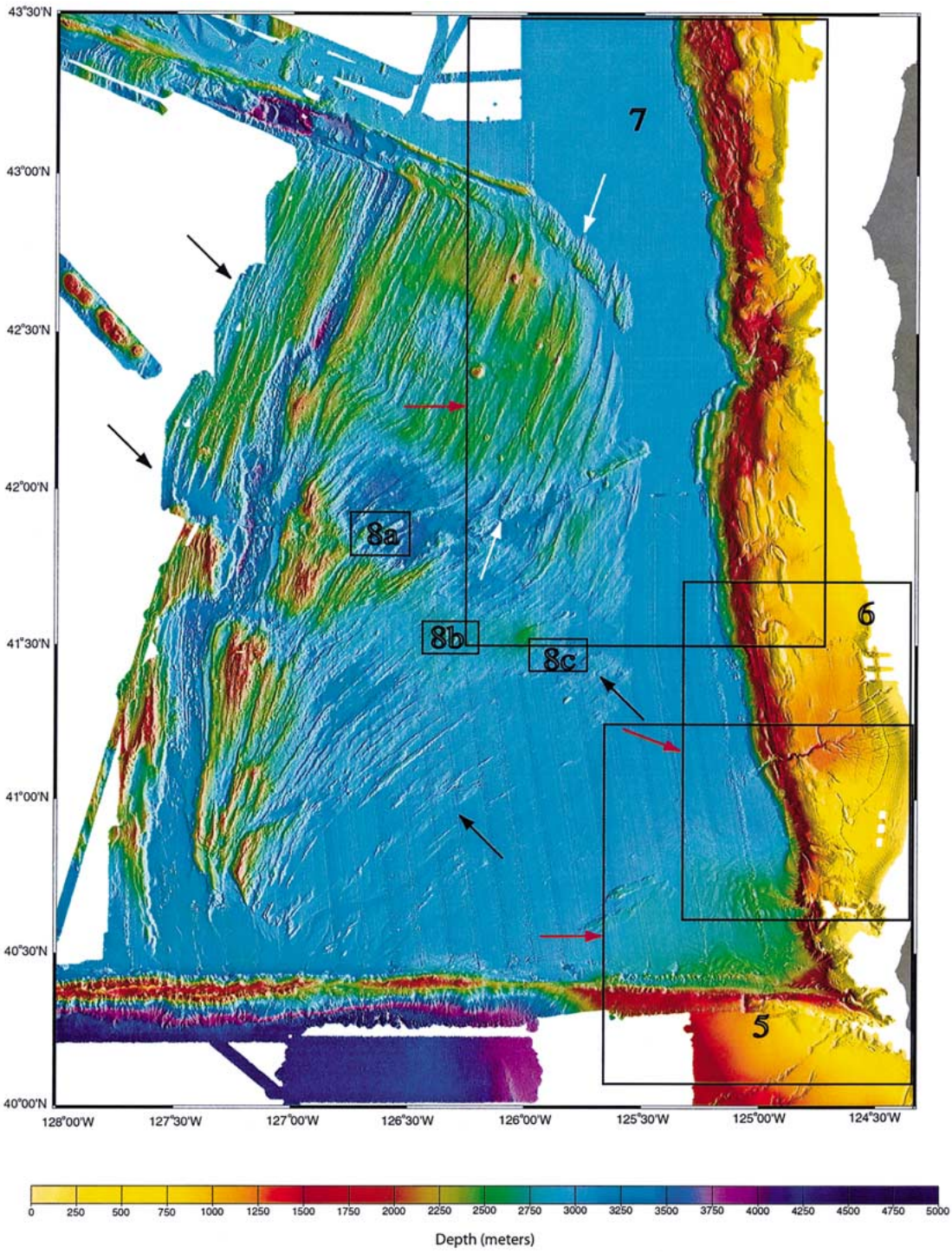

Figure 4. Large-scale map of the Gorda Plate. Boxes are locations of the 3-dimensional perspectives shown in Figures 5, 6, and 7, and the right-lateral offsets highlighted in Figure 8a, b, c. Red arrows in the boxes show the origin and look directions of the figures. White arrows show the locations of NE to NNE trending faults that are likely re-activated spreading-fabric normal faults since they parallel magnetic anomaly trends. Black arrows show locations of the northwest trending bands of discordant lineations (corresponding to shallow basins) discussed in text.

Table 1. SeaBeam Swath Bathymetry Data Sources.

Years	Ship(s)	Swath Mapping System	Number of Cruises	Primary Navigation	Coverage area (10^8 m^2)
1980–1984 1986–1989	Surveyor Discoverer	SeaBeam	11	Loran-C	112.458
1984–1991	Surveyor	SeaBeam (EEZ)	26	RAYDIST/ ARGO	220.844
1984; 1988	Davidson	BS^3	4	RAYDIST/ ARGO	209.580
1994–1995 1995	Laney Chouest Surveyor/Disco.	SeaBeam	6	GPS	45.457
1997	Brown	SeaBeam 2100	1	GPS	513.293

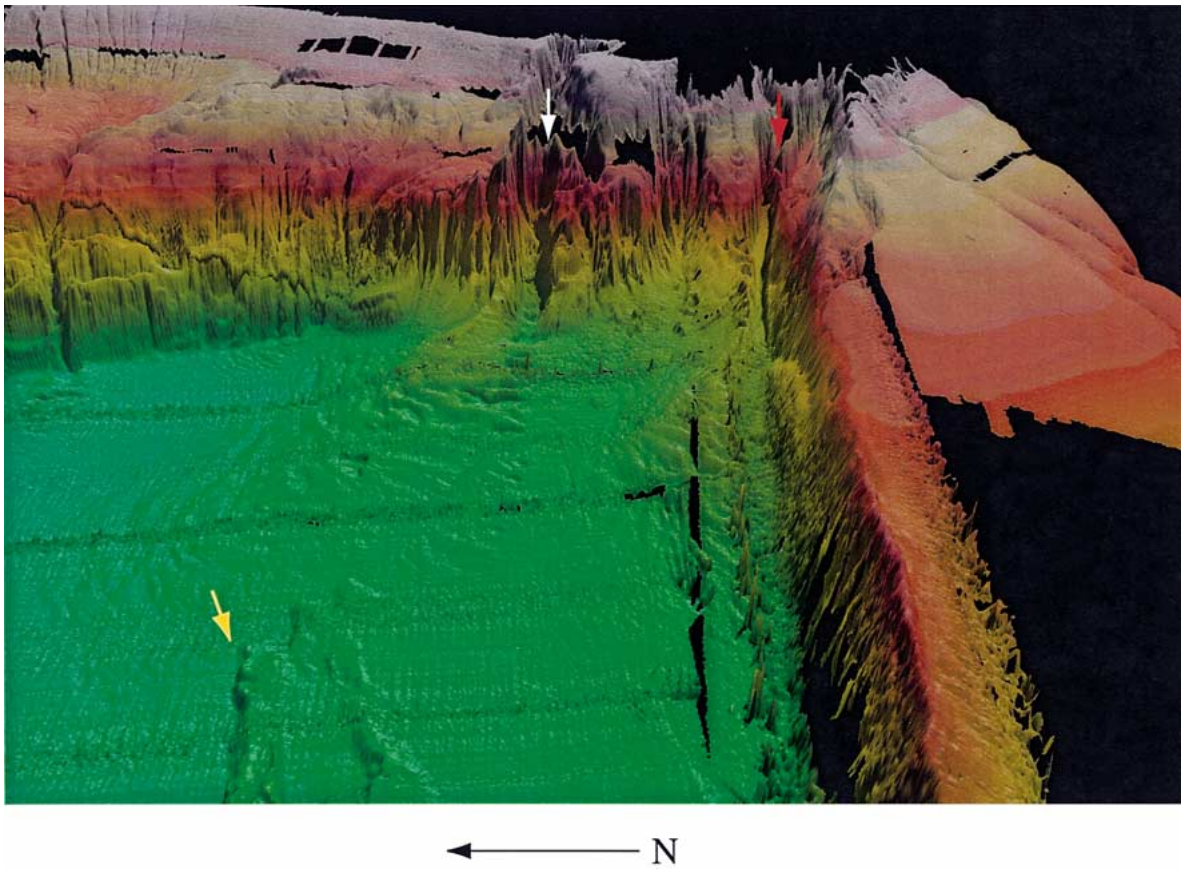

Figure 5. Three-dimensional perspective map of the Mendocino and Eel Canyons showing development of the proximal sediment fans at the mouths of the canyons. View azimuth is from the northwest. The two fans that formed at the bases of the Eel (white arrow) and Mendocino Canyons (red arrow) coalesce into one large fan extending several kilometers into the Gorda Plate abyssal plain. The northwest portion of the fan is offset by two large NE-SW trending scarps in the foreground (yellow arrow).

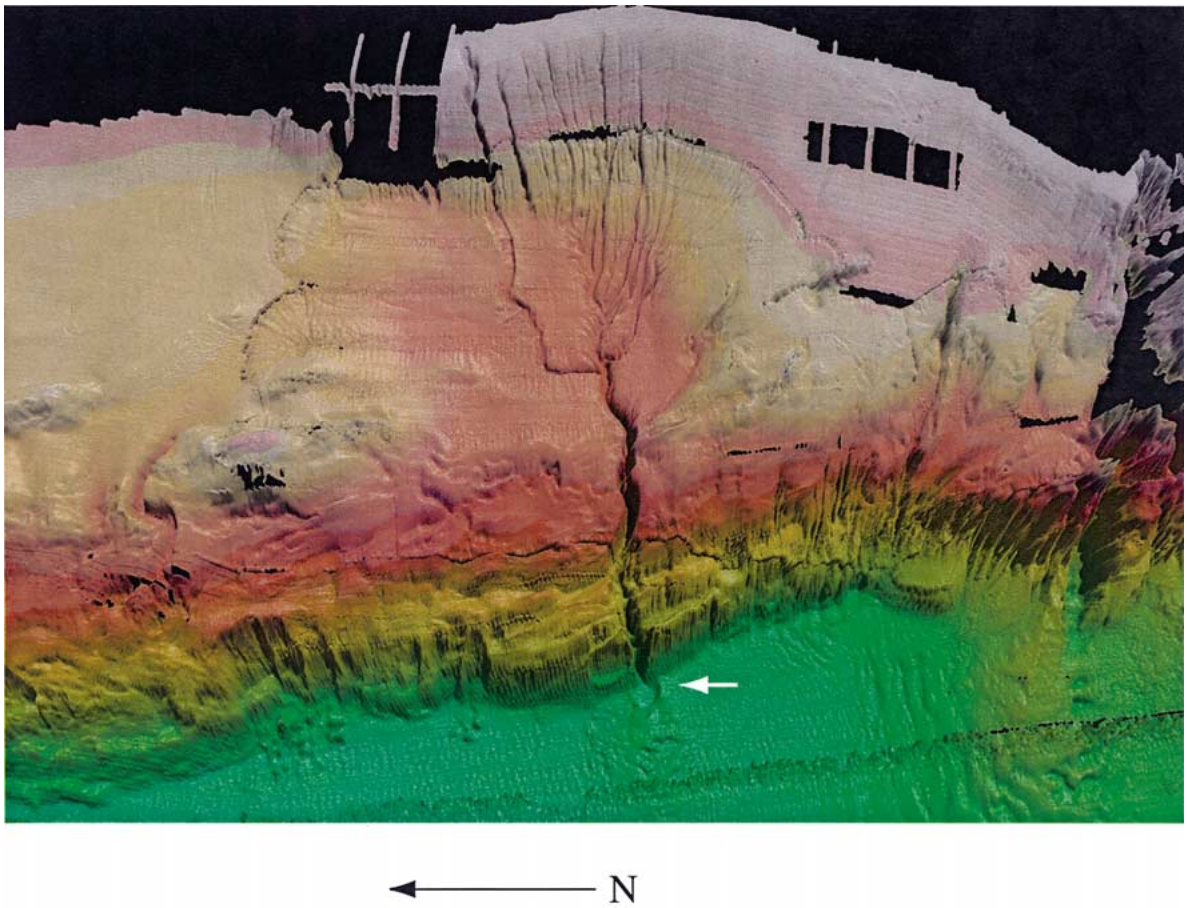

Figure 6. Three-dimensional perspective map of the Trinidad Canyon, plunge pool, and forearc basin at the head of the canyon. The Trinidad Canyon and forarc basin are readily evident in the margin morphology, with a large ~10 km plunge pool (white arrow) formed at the mouth of the canyon as it enters the Gorda Plate sediments. Presumably the plunge pool formed as turbidity currents exited the canyon at a shallow depth in the margin, then sank rapidly and impacted the abyssal plain sediments.

processing. The outer 10–20 beams on individual pings typically have return times that are significantly longer than expected (and hence deeper) than the inner 80–100 beams based on the depth measured from the center beam. This results in the appearance of along-track troughs on both sides of the swath, readily apparent in the bathymetry along the southeastern portion of the Gorda Plate (Plate 1). Varying the swath width from 10 to 6 km did reduce, but not eliminate, the problem. Employing different sound-speed profiles also proved ineffective. The multibeam data were initially collected using ocean sound-speed models of the region available from the Generalized Digital Environmental Model (Davis et al., 1986). The GDEM is the result of 30 years of direct sampling of ocean sound velocity parameters (temperature, salinity, and pressure) and accounts for seasonal variation. This outer beam problem is most obvious in deeper, smoother sections of the seafloor. Rough and more shallow seafloor terrain seems to alleviate (or simply make less obvious) the problem, probably because the rough terrain more effectively scatters echo energy back to the hydrophones allowing for a more accurate timing of the peak return amplitude.

Other errors are evident in the small-scale maps. The depth differences between the multibeam surveys in the 1980s and the more recent surveys in the 1990s are apparent in Figures 5–7, as well as data gaps when surveys were non-overlapping. Also, several parallel "ruts" are present in the bathymetry along the toe of the accretionary wedge (Figures 5–7). These comb-like ruts are artifacts present in multibeam surveys from both the 1980s and 1990s. The ‘ruts’ are likely due to the inability of the multibeam system to re-

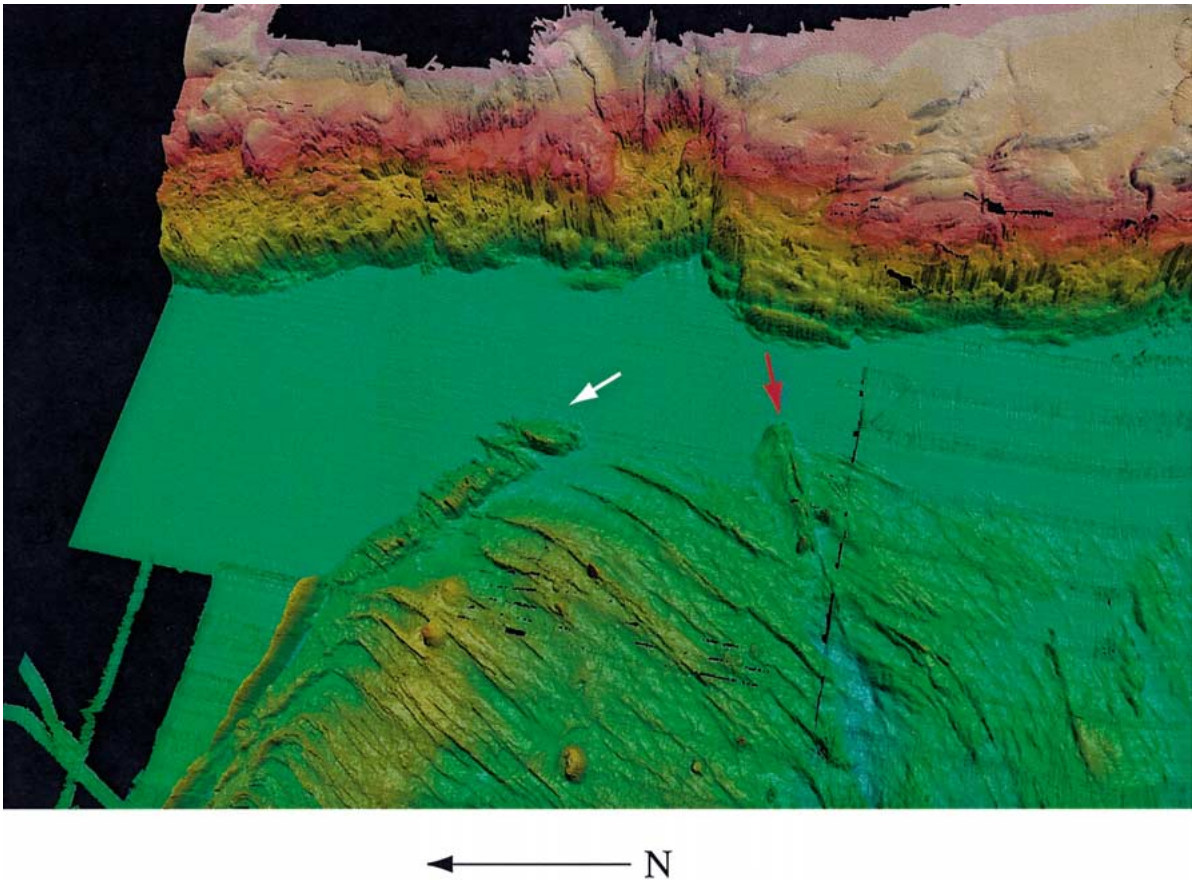

Figure 7. Three-dimensional perspective map of the continental margin where the intersection of two pseudofaults correlates with a right-step in the strike of the toe of the margin. The two pseudofaults form prominent bathymetric ridges, deform young sediments and show substantial vertical, and some horizontal, separation. The first pseudofault is located in the northern part of the Gorda Plate and trends NW-SE (white arrow) from the end of the Blanco Fracture Zone. The second pseudofault trends NE-SW and is located along the center of the plate (red arrow). Both pseudofaults become buried by sediments as they continue eastward along the subducting slab, and align with an indentation in the continental margin, with their intersections possibly correlating with a right step in the trend of the toe of the margin.

solve consistent depths from the steep terrain along the edge of the continental margin. Additionally, the ruts may be due to strong (near-specular) backscatter from the margin slope contaminating the signal in the other beams (i.e., the side-lobe artifact discussed in de Moustier and Kleinrock, 1986).

Significant Morphologic Features

Overall, the new multibeam bathymetry illustrates the complex structure of the Gorda Plate from its origin at the rift grabens along the Gorda Ridge to its termination along the transverse ridge bounding the Mendicino Transform Fault and beneath the deformed sediments of the continental margin. The volcanic nature of the Gorda Ridge is evident in Plate 1 from the presence of ubiquitous volcanic cones along the rift valley floor. Also apparent is the dominant role sediment deposition from the Columbia and other major rivers along the Pacific Northwest coast plays in defining the morphology of the seafloor. The major structural elements of the Gorda Plate near the continental margin are buried by sediment, as is the southernmost Gorda Ridge. Several drainage channels that presumably fed the sediment deposition along the southern part of the plate are evident in the bathymetry (Plate 1).

The complete multibeam bathymetric data have revealed several major, previously unmapped faults. A series of gently curving faults are apparent in the Gorda Plate, with numerous faults offsetting the Gorda Plate seafloor (Plate 1). Pliocene and younger faults have been previously mapped in a small section of

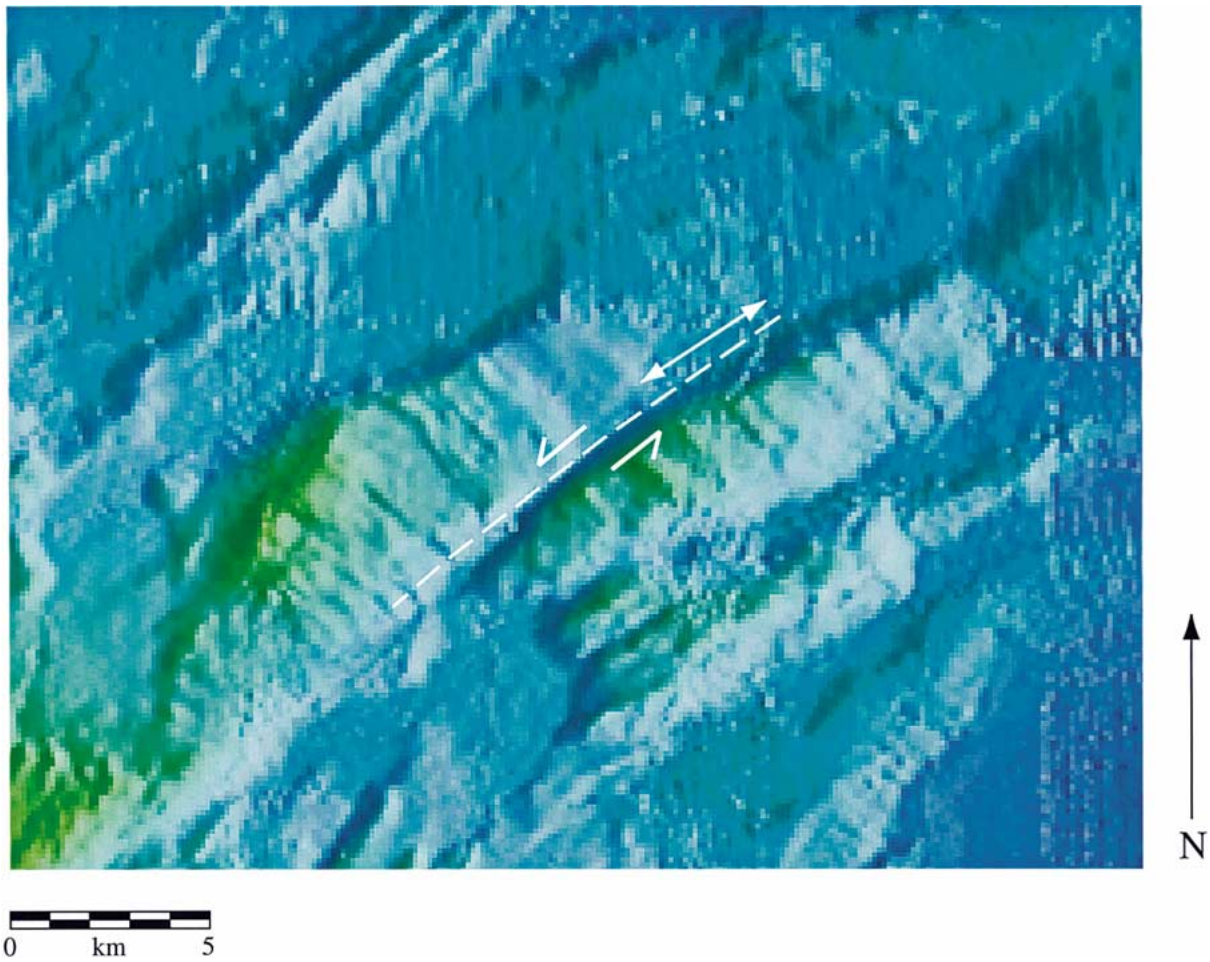

Figure 8. Examples of left-lateral separation of the southern limb of the Gorda flexural buckle. See Figure 4 for locations. Dashed line shows approximate trend of the fault, arrows indicate the interpreted offset.

the northern Gorda Plate using seismic reflection and Gloria sidescan data, as well as some of the multibeam bathymetry data presented here (Goldfinger et al., 1992). These Gorda Plate faults trend NE to NNE (Figure 4) and are likely re-activated spreading-fabric normal faults since they are parallel to the trend of the magnetic anomalies (Figure 2). Although these basement faults seem to show uplift to the west (Goldfinger et al., 1992), it is not clear if the faults are normal or reverse, or how much of a component of strike-slip motion is involved.

The first-order structural trends apparent from the bathymetry (Figure 4; Plate 1) indicate the Gorda Plate basement-fabric faults are likely relict spreading fabric faults since they are parallel to the trend of the northern Gorda Ridge axial valley faults. Tracing the faults southward, however, they become significantly oblique to the ridge south of 42°15′ N. The basement faults to the south continue to rotate clockwise with distance east from the ridge axis until the fabric is buried by the abyssal plain sediments. The faults in the south are also probably relict fabric faults since they are in most instances still connected (traceable) to the ridge parallel faults in the north and the overall pattern in the basement fabric parallels the shape of the magnetic lineations (Figure 2). Indeed the overall sinusoidal shape of the fabric faults is presumably a product of the intense N-S compressional stress environment of the Gorda Plate (Stoddard, 1987; Wilson, 1989) as it is squeezed between North America and the Pacific Plate. Furthermore, the bathymetry data indicate there are two northwest trending linear basins in the west-central part of the plate (black arrows in Figure 4). These linear basins have been interpreted

Figure 8. (Continued)

as right-lateral shear zones based on Gloria sidescan data (Wilson, 1989), and are juxtaposed with right-lateral offsets in the Gorda Ridge at 41°40′ N and at 42°25′ N (Masson et al., 1988). The northwest trending basins are even apparent on the western flank of the Gorda Ridge: the 42°25′ N as a very slight curve in the basement fabric, and the 41°40′ N as a well-developed basin (Figure 4). This implies that these two features reflect deformation occurring across the Gorda Plate, Gorda Ridge, and perhaps into the Pacific Plate. However from Figure 4 and Plate 1, the basement ridges appear to bend smoothly through these basins and do not show a distinct fault offset. Therefore, it could be that these linear basins reflect either right-lateral shear at depth, or may be due to flexural folding of the plate in response to the N-S compressional deformation.

The Mendocino and Eel Canyons are prominent morphologic features in the northern California margin (Figure 5). These canyons are apparently active depositional features. Indeed, following a large ($M_w = 6.6$) earthquake in 1992 off Cape Mendocino, a turbidity current flowed through Mendocino Canyon breaking a submarine cable deployed across the canyon (Dziak et al., 1997). A large sediment fan is present at the mouths of the Mendocino and Eel fans which probably formed by coalescence of two fans. The depositional lobes of the fan(s) are evident in the bathymetry, as are the turbidite channels that have deposited sediment along the fans over time. It appears that the northwestern section of the fan is truncated by a prominent ridge (Figure 5). This ridge was interpreted as a fault scarp (Trehu et al., 1995) from multichannel seismic records and coincides with the aftershock zone of a large ($M_S = 7.3$) earthquake that occurred in the southeastern section of the Gorda Plate (41°9.0′ N; −124°18.0′ W) on November 8, 1980. Thus cores of fan sediments along this fault scarp may show geologic evidence of large earthquakes in the past.

The Trinidad Canyon and an apparent plunge pool are shown in Figure 6. The Trinidad Canyon is readily evident in the margin morphology, with a large (∼10 km) plunge pool formed at the mouth of the canyon as it enters the Gorda Plate sediments. Presumably the plunge pool formed as turbidity currents exited the canyon at a shallow depth in the margin, then sank rapidly and impacted the abyssal plain sediments. The absence of a proximal sediment fan at the end of the Trinidad Canyon suggests sediment loads are much less than the Mendocino and Eel Canyons, but this also may be a result of the depositional environment that produced the plunge pool. The large basin at the head of Trinidad Canyon shows it to be a major drainage system along this section of the con-

Figure 8. (Continued)

tinental margin. Similar basins are observed in the forearc along the Nankai Trough (Sugiyama, 1992). The Nankai Trough forearc basins are thought to arise from compression across the forarc resulting from oblique subduction, with each basin representing individual rupture segments of the subducting oceanic plate during large interplate earthquakes. The forearc basin above the Trinidad Canyon may have a similar origin, and therefore may reflect a discrete structural segment of the Gorda Plate that would limit the rupture extent of large subduction zone earthquakes.

Two pseudofaults are readily apparent in the bathymetry and form prominent bathymetric features. These pseudofaults were first identified from the magnetic anomaly data by Wilson (1993), but can be more precisely located from the bathymetry presented here. Both pseudofaults deform young sediments and show substantial vertical, and some horizontal, separation. The first pseudofault (Figure 2) is located in the northern part of the Gorda Plate and trends NW-SE from the end of the Blanco Fracture Zone (Figure 7 – white arrow). The second pseudofault trends NE-SW and is located along the center of the plate (Figure 7 – red arrow). Based on interpretation of EEZ 2-channel reflection data (Goldfinger et al., 1992), this second pseudofault has apparently been re-activated as a reverse fault. Both pseudofaults become buried by sediments as they continue eastward along the subducting slab. Both also align with a prominent indentation in the continental margin, with their intersections apparently correlating with a right step in the trend of the toe of the margin. It seems clear from these observations that pseudofaults can indeed become actively moving faults as stress distributed throughout the plate causes slip along pre-existing zones of weakness. The intersection of the pseudofaults, since they likely are reflecting offsets in the Gorda Plate basement, may also constitute another segment boundary along the subducting plate.

Tectonic Deformation Model

The complete multibeam coverage of the Gorda Plate allows for some new constraints on the kinematic models of Gorda Plate deformation. Several models of the deformation history and current stress regime within the Gorda Plate have been proposed over the years (Bolt et al., 1968; Riddihough, 1980; Knapp, 1982; Stoddard, 1987, 1991 Masson et al., 1988; Wilson, 1989). The deformation analyses done in these studies were based on matching the relatively low resolution magnetic data (Figure 2), augmented in some cases by fault analysis of the regional Gloria sides-

can data (EEZ-SCAN, 1986). Most of these models used the development of large scale strike-slip faults to account for the apparent offset, or curvature, of the magnetic lineations. Although Masson et al. (1988) invoked blurring in the magnetic record to account for the curvature of the anomalies and suggested the Gloria data showed no curved fault lineations. Alternatively, a model proposed by Silver (1971), then modified by Stoddard (1987), invoked flexural-slip buckling as the source of the magnetic lineation curvature and assumed widely distributed deformation along pre-existing zones of weakness inherited from the ridge. The magnetic lineations have the appearance of a half sinusoid (Figure 2). The absence of a full waveform may result from obduction of Gorda Plate crust onto the Mendocino Ridge (Stoddard, 1987). Recent submersible observations and dated samples from the Mendocino Ridge suggest it is comprised principally of Gorda Plate material, and that the ridge has been raised above sea level during possible obduction events (Fisk et al., 1993). This is supported by the presence of wavecut platforms with rounded cobbles now at the ridge flanks at ∼1800 m depth.

From Figure 4 and Plate 1, it is now clear that the pervasive basement ridges seen in the Gorda Plate are smoothly curved, similar to the magnetic lineations, and are for the most part not offset by strike-slip faults cutting across the basement fabric. It is possible that small strike-slip offsets along a multitude of faults, each with a total slip less than the 100-m resolution of the bathymetric data, could produce the same effect, although it does not seem likely. In some areas, the basement fabric is not smoothly curved but 'kinked' (Plate 1). In other regions, there appear to be large wavelength folds that gently bend the basement fabric. Furthermore, the basement lineations appear to be drag folded adjacent to pseudofaults that may have been activated as tectonic structures (Goldfinger et al., 2000).

There is evidence of strike-slip offsets along the curved linear ridges parallel to the strike of the basement fabric (Figures 8a, b, c). The linear ridges vary considerably in height along strike, and the exposed highs are offset in the along strike direction. This faulting style appears to be pervasive, and only seems to occur in the southern part (south of $\sim 42°30'$ N) of the Gorda Plate. Although the large amount of sediment cover on top of the southern part of the plate seems to play a role in making identification of ubiquitous sinistral faulting difficult. Furthermore, there is not convincing evidence of strike-slip motion in the northern Gorda Plate which appears to be moving passively with the remainder of the Juan de Fuca Plate (Figure 4 and Plate 1). In effect, the Gorda Plate appears to be deforming similar to a large-scale flexural-slip fold (Yeats, 1986) as viewed in cross-section (Figure 9; Goldfinger et al., 2000). In a flexural fold, opposing limbs have opposite senses of motion and separation is reduced near the axis. However, in the case of the Gorda Plate, the northen limb is apparently fixed while the southern limb is slipping along bedding planes, thus giving the plate the overall appearance of a monocline or even a large-scale drag fold. This model is consistent with elements of Gorda Plate deformation histories proposed by Wilson (1989) and Stoddard (1987). Wilson (1989) proposed that deformation only occurs in the southern part of the Gorda Plate and is distributed along NE-SW faults away from the ridge, while Stoddard (1987) suggested sinistral motion occurs along the southern section of the Gorda Plate (as well as dextral-slip within the northern section) with deformation accommodated by faults parallel to the magnetic anomalies.

The deformation model presented here is based on a first-order analysis of the newly available bathymetric data. The structural model of the Gorda Plate, however, needs to be rigorously tested and several key supporting data sets are required. An effort is currently underway to re-survey several important deformation features within the Gorda Plate with DSL-120 sidescan sonar, a 4.5 KHz sub-bottom profiler, and a high-resolution multi-channel seismic system. Age constraints on the timing of deformation will be obtained from the analysis of several piston cores to be collected throughout the Gorda abyssal plain, and from age stratigraphy based on the recently drilled ODP site 1020 in the abyssal plain along the southeast section of the Gorda Plate. Furthermore, active fault zones and the Gorda intraplate stress regime will be identified by combining microearthquake ($M < 3.5$) locations derived from hydrophone arrays deployed throughout the northeast Pacific Ocean (Fox and Dziak, 1999) with fault-plane solutions of moderate-sized ($M > 3.5$) earthquakes derived from moment-tensor inversion of regional broadband land-based seismic data from stations throughout the Pacific Northwest (Nabelek and Xia, 1995). Combination of these data sets should allow for the development of a robust kinematic model of Gorda Plate deformation.

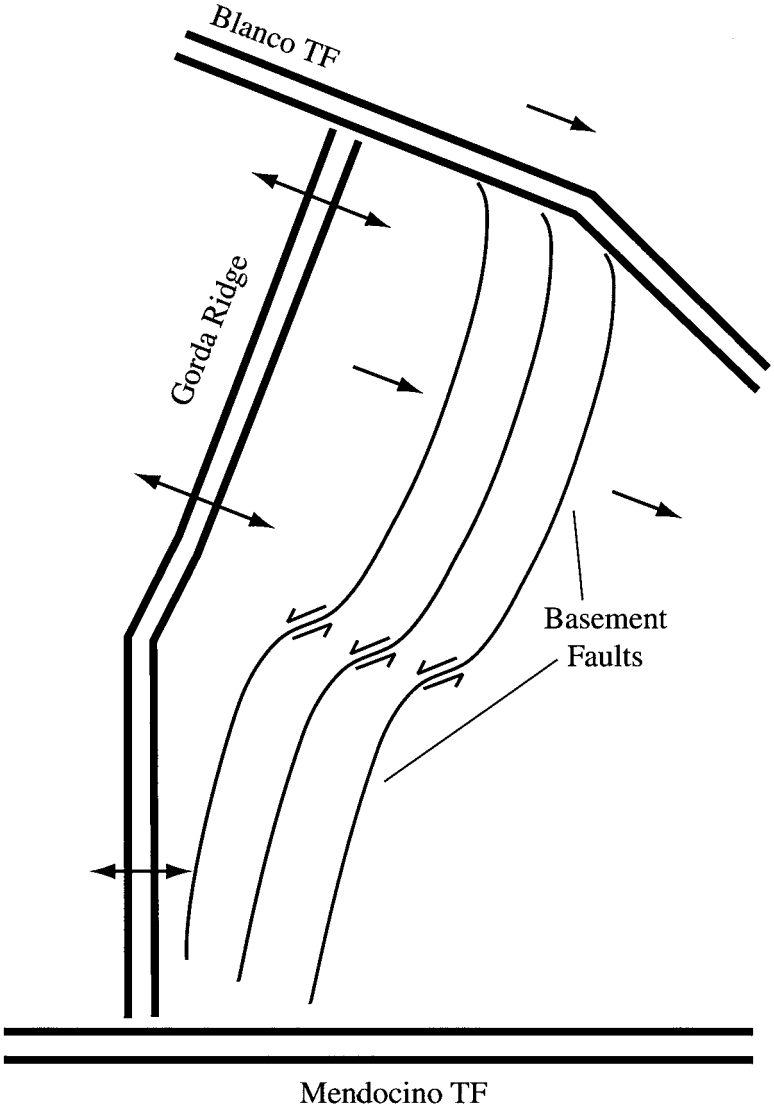

Figure 9. Line drawing of the structural interpretation for the deformation of the Gorda Plate based on offsets observed in the SeaBeam bathymetry presented. Left slip is observed in the southern section of the Gorda Plate, while the northern section appears to be moving passively with the Juan de Fuca Plate. Model is consistent with those proposed by Wilson (1989) and Stoddard (1987).

Summary

Although there are clearly recognized inadequacies within the data, full-coverage multibeam bathymetry maps of an entire tectonic plate can provide a wealth of information, based on seafloor morphology alone, for a variety of volcanological, tectonic, and sedimentological processes. The 20-year compilation of bathymetry illustrates the complex structure of the Gorda Plate from its origin at the rift grabens along the Gorda Ridge to its termination along the transverse ridge bounding the Mendicino Transform Fault and beneath the deformed sediments of the continental margin. The volcanic nature of the Gorda Ridge is evident from the presence of ubiquitous volcanic cones along the rift valley floor. Additionally, the bathymetric data have revealed several major, previously unmapped midplate faults. A series of gently curving faults are apparent in the Gorda Plate, with numerous faults offsetting the Gorda Plate seafloor. The multibeam surveys also provide a detailed view of the intense deformation occurring within the Gorda Plate. A preliminary deformation model estimated from basement structure suggests the southern part of

the plate (south of $\sim$ 42°30′ N) may be deforming through a series of left-lateral strike-slip faults, while the northern section appears to be moving passively with the rest of the Juan de Fuca Plate. The bathymetry also demonstrates the Mendocino and Eel Canyons are prominent morphologic features in the northern California margin. These canyons are active depositional features with a large sediment fan present at the mouths of both the Mendocino and Eel canyons. This single fan probably formed by coalescence of fans from each canyon. The depositional lobes of the fan(s) are evident in the bathymetry, as are the turbidite channels that have deposited sediment along the fans over time. The Trinidad Canyon is readily evident in the margin morphology as well, with a large ($\sim$10 km) plunge pool formed at the mouth of the canyon as it enters the Gorda Plate sediments.

Recently, the NEPTUNE project was established to create a network of seafloor observatories distributed throughout the Juan de Fuca Plate that are linked to each other, and shore stations, by a system of high-speed, submarine communication-control links using fiber-optic/power cables. The bathymetry of the Gorda Plate presented here can provide the basis for observatory and cable site selection, as well as contribute a baseline of bathymetric data for comparison to future multibeam surveys. In addition, the recently created Global Ocean Mapping Project (GOMaP) proposes development of a long-term international effort to map the world ocean floor using, at least initially, hull-mounted or possibly towed sidescan/swath bathymetric systems (Vogt et al., 2000). It is the goal of GOMaP to produce a seafloor backscatter image whose lowest spatial resolution, in the deep trenches, would be at least about 100 m. In support of the GOMaP effort, we think the Gorda Plate bathymetry presented here demonstrates the usefulness of collecting good resolution, plate-scale multibeam data for addressing a wide range of geological and geophysical research topics.

Acknowledgements

The authors would like to thank the officers and crew of the NOAA Ships *Discoverer*, *Surveyor*, *Davidson*, *Ronald H. Brown*, and the R/V *Laney Chouest*. Their outstanding work at sea made completion of this study possible. Figures 4, 8, and Plate 1 were produced using the Generic Mapping Tool (Wessel and Smith, 1998). Figures 5–7 were made using the Fledermaus 3-D visualization software (Mayer et al., 2000). Funding and facilities provided by the NOAA VENTS program, PMEL contribution number 2242.

References

Bolt, B. A., Lomnitz, C. and McEvilly, T. V., 1968, Seismological evidence on the tectonics of central and northern California and the Mendocino Escarpment, *Bull. Seism. Soc. Am.* **58**, 1725–1767.

Clarke, S. H., Jr. and Carver, G. A., 1992, Late Holocene tectonics and paleoseismicity, southern Cascadia Subduction Zone, *Science* **255**, 188–192.

Cochran, J. R., Goff, J. A., Malinverno, A., Fornari, D. J., Keeley, C. and Wang, X., 1993, Morphology of a 'Superfast' Mid-Ocean Ridge crest and flanks: The East Pacific Rise, 7°–9° S, *Mar. Geophys. Res*. **15**, 65–75.

Davis, T. M., Countryman, K. A. and Carron, M. J., 1986, Tailored acoustic products utilizing the NAVOCEANO GDEM (a generalized digital environmental model), in *Proceedings, 36th Naval Symposium on Underwater Acoustics*, Naval Ocean Systems Center, San Diego, CA.

De Moustier, C. and Kleinrock, M. C., 1986, Bathymetric artifacts in Sea Beam data: How to recognize them and what causes them, *J. Geophys. Res.* **91**, 3407–3424.

Denlinger, R., 1992, A Model for Large-scale plastic yield of the Gorda Deformation Zone, *J. Geophys. Res*. **97**, 15415–15423.

Dziak, R. P., Fox, C. G., Matsumoto, H. and Schreiner, A. E., 1997, The April 1992 Cape Mendocino earthquake sequence: Seismo-acoustic analysis utilizing fixed hydrophone arrays, *Mar. Geophys. Res*. **19**, 137–162.

EEZ-SCAN 84 Scientific Staff, 1986, Atlas of the Exclusive Economic Zone, western conterminous United States, scale 1:500,000, Miscellaneous Investigations Series I-1972, U.S. Geological Survey.

Fisk, M. R., Duncan, R. A., Fox, C. G. and Witter, J. B., 1993, Emergence and petrology of the Mendocino Ridge, *Mar. Geophys. Res*. **15**, 283–296.

Fox, C. G. and Dziak, R. P., 1999, Internal deformation of the Gorda Plate observed by hydroacoustic monitoring, *J. Geophys. Res*. **104**, 17603–17615.

Goldfinger, C., Dziak, R. P. and Fox, C. G., 2000, Kinematic model for the deformation of the Gorda Plate based on Seabeam bathymetry, *Geology* (in preparation).

Goldfinger, C., Kulm, L. D. and Yeats, R. S., 1992, Neotectonic map of the Oregon continental margin and adjacent abyssal plain, Oregon Department of Geology and Mineral Industries, Open-File Report, O-92-4, scale 1:500,000.

Knapp, J. S., 1982, Seismicity, crustal structure, and tectonics near the northern termination of the San Andreas Fault, Ph.D. Thesis, University of Washington, Seattle, pp. 343.

Lay, T., Given, J. W. and Kanamori, H., 1982, Long-period mechanism of the 8 November 1980 Eureka, California, earthquake. *Bull. Seism. Soc. Am*. **71**, 1–24.

Macdonald, K. C., Fox, P. J., Miller, S., Carbotte, S., Edwards, M. Eisen, M., Fornari, D. J., Perram, L., Pockalny, R., Scheirer, D., Tighe, S., Weiland, C. and Wilson, D., 1992, The East Pacific Rise and its flanks 8°–18° N: History of segmentation, propagation, and spreading direction based on SeaMARCII and SeaBeam studies, *Mar. Geophys. Res*. **14**, 299–344.

Mason, R. G. and Raff, A. D., 1961, A magnetic survey off the west coast of North America 32° N to 42° N, *Geol. Soc. Am. Bull*. **72**, 1259–1265.

Masson, D. G., Cacchione, D. A. and Drake, D. E., 1988, Tectonic evolution of the Gorda Ridge inferred from sidescan sonar images, *Mar. Geophys. Res*. **10**, 191–204.

Mayer, L. A., Paton, C. W., Gee, L, Gardner, J. V. and Ware, C. W., 2000, Interactive 3-D Visualization: A tool for seafloor navigation, exploration, and engineering, *Proceedings of the IEEE Oceans*, Vol. 2., pp. 913–920.

Nabelek, J. L. and Xia, G., 1995, Moment-tensor analysis using regional data: Application to the Scotts Mills, Oregon earthquake, *Geophys. Res. Lett*. **22**, 13–16.

Purdy, G. M., Sempere, J.-C., Schouten, H., Dubois, D. L. and Goldsmith, R., 1990, Bathymetry of the Mid-Atlantic Ridge, 24°–31° N: A map series, *Mar. Geophys. Res*. **98**, 13835–13850.

Riddihough, R. P., 1980, Gorda plate motions from magnetic anomaly analysis, *Earth Planet. Sci. Lett.* **51**, 163–170.

Riddihough, R. P., 1984, Recent plate motions, *JFP-9, Open File Report 83-6*, Pacific Geoscience Center, Earth Phys. Branch, Sidney, B.C., Canada.

Scheirer, D. S., Macdonald, K. C., Forsyth, D. W., Miller, S. P., Wright, D. J., Cormier, M.-H. and Weiland, C. M., 1996, A map series of the southern East Pacific Rise and its flanks, 15° S to 19° S., *Mar. Geophys. Res*. **18**, 1–12.

Silver, E. A., 1971, Tectonics of the Mendocino Triple Junction, *Geol. Soc. Am Bull.* **82**, 2965–2978.

Smith, S. W., Knapp, J. S. and McPherson, R. C., 1993, Seismicity of the Gorda Plate, structure of the continental margin, and an eastward jump of the Mendocino Triple Junction, *J. Geophys. Res*. **98**, 8153–8171.

Spence, W., 1989, Stress origins and earthquake potentials in Cascadia, *J. Geophys. Res.* **94**, 3076–3088.

Stoddard, P. R., 1987, A kinematic model for the evolution of the Gorda Plate, *J. Geophys. Res.* **92**, 11524–11532.

Stoddard, P. R., 1991, A comparison of brittle deformation models for the Gorda Plate, *Tectonophys.* **187**, 205–214.

Sugiyama, Y., 1992, The cenozoic tectonic history of the forearc region of southwestern Japan, based mainly on data from the Shizuoka district, *Bull. Japan. Geol. Surv*. **43**, 91–112.

Trehu, A., Lendl, C., Leitner, B., Meltzer, A., Gulick, S., Holl, J., Levander, A., Henstock, T., Beaudoin, B., Godfrey, N., Hole, J., Klemperer, S. Clarke, S., Luetgert, J., Mooney, W. D., 1995, Pulling the rug out from under California: Seismic images of the Mendocino Triple Junction, *Eos Transactions, American Geophysical Union* **76**, 380–381.

Velasco, A. A., Ammon, C. J. and Lay, T. 1994, Recent large earthquakes near Cape Mendocino and in the Gorda Plate: Broadband source time functions, fault orientations, and rupture complexities, *J. Geophys. Res*. **99**, 711–728.

Vine, F. J. and Mathews, D. H., 1963, Magnetic anomalies over oceanic ridges, *Nature* **199**, 947–949.

Vogt, P. R., Jung, W.-Y. and Nagel, D. J., 2000, Global Ocean Mapping Project (GOMaP): A matchless resolution to start the new millennium, Eos Transactions, *American Geophysical Union* **81** (23), 254–258.

Wang, K., He, J. and Davis, E. E., 1997, Transform push, oblique subduction resistance, and intraplate stress of the Juan de Fuca Plate, *J. Geophys. Res*. **102**, 661–674.

Wessel, P. and Smith, W. H. F., 1998, New, Improved version of the Generic Mapping Tools released, *EOS Transactions, AGU* **79**, 579.

Wilson, D., 1989, Deformation of the so-called Gorda Plate*, J. Geophys. Res*. **94**, 3065–3075.

Wilson, D., 1993, Confidence intervals for motion and deformation of the Juan de Fuca Plate, *J. Geophys. Res.* **98**, 16053–16071.

Yeats, R. S., 1986, Active faults related to folding, in Wallace, R.E. (ed.), *Active Tectonics*, National Academy Press, Washington DC, pp. 63–79.